

Free Electron Theory for Thin Metal Films

Philip B. Allen^{1,*}

¹*Department of Physics and Astronomy, Stony Brook University,
Stony Brook, New York 11794-3800, USA*

(Dated: June 25, 2024)

Quantum free electrons, *i.e.* plane waves, with wavevector \vec{k} , and occupancy constrained by the Pauli exclusion principle, are explained in all introductory texts about solids. A free-electron description works surprisingly well for many properties of “simple” metals. It is assumed that the interior of the metal is essentially infinite, and surfaces are presumed irrelevant. Over the past 30 years, experiments that visualize surfaces have revolutionized solid state physics, stimulating new theory and applications. Therefore, a basic question is, how can the free electron picture be applied to properties of solids where surfaces play a prominent role? Various versions of an extended free-electron theory are used, but not always explained pedagogically. This paper focusses on idealized metallic films. Three versions (an oversimplified one and two stages of improvement) of a free-electron description of metal films are given. These versions are illustrated in detail for the specific example of a slab of aluminum with six layers of atoms.

I. INTRODUCTION

Not long after the electron was discovered and recognized as a particle, Drude [1] showed a way to understand electrical conduction in metals using a classical description of electrons wandering freely (except for occasional scattering) in a homogeneous medium. Atoms, and electrical charge, are ignored. In the early days of quantum mechanics, Sommerfeld [2] gave the quantum version of Drude’s model. The free-electron wave functions used in this “Drude-Sommerfeld model” are

$$\psi_{\vec{k}} = \frac{1}{\sqrt{V}} e^{i\vec{k}\cdot\vec{r}} = \frac{1}{\sqrt{V}} e^{i(k_x x + k_y y + k_z z)} \quad (1)$$

where V is the volume of the metal. The state \vec{k} has energy

$$\epsilon_{\vec{k}} = \frac{\hbar^2 |\vec{k}|^2}{2m} \quad (2)$$

as follows from the Schrodinger equation for a non-relativistic electron of mass m and no interactions, $\mathcal{H} = p^2/2m$. Since electrons obey Fermi statistics, the Pauli exclusion principle applies, and quantum states $\psi_{\vec{k}}$ can be occupied by at most one electron of spin up and one of spin down. The set of vectors \vec{k} is known as “reciprocal space,” or \vec{k} -space. This picture gives a surprisingly useful model of bulk behavior of “simple metals” (like Na, Mg, Al, and Pb), in situations where surfaces can be ignored.

Thin crystalline films have become increasingly important in the last 30 years, stimulated

by the invention of the scanning tunneling microscope [3, 4]. This led to remarkable improvements in film growth, new visualizations and spectroscopies, and new applications. The free-electron description can be modified to describe how electrons behave in films of simple metals where the surfaces parallel to the films can no longer be ignored. In metallic films, electrons propagate freely in two dimensions, parallel to the film, but have discrete “quantum well states” (QWS’s) in the perpendicular direction. The experimental spectra shown in Fig. 1 contain evidence of QWS’s evolving with film thickness. Such effects have been studied by experiment and theory [5–8], and treated pedagogically [9–11]. The aim of the present article is to go deeper into the pedagogy and explore deeper extensions of the free-electron model.

II. PERIODIC BOUNDARY CONDITIONS

In Eq. 1 the plane wave state $\psi_{\vec{k}}$ is normalized so that $\int_V d\vec{r} |\psi_{\vec{k}}(\vec{r})|^2 = 1$. A finite volume V is used, but apart from normalization, $\psi_{\vec{k}}$ appears, at first sight, unaltered by the boundary. There is, however, an important alteration: the wavevector \vec{k} is discretized.

Actual boundaries do alter the wave function, and destroy the propagating wave nature close to the boundary. This is correctly ignored when the aim is to describe bulk properties. But discretization of \vec{k} is necessary to quantify the number of states $\psi_{\vec{k}}$ available for the electrons contained in V . This is done by “periodic boundary conditions” (periodic BC’s), introduced by Born and von Karman [13] in 1912.

Consider a finite but otherwise perfect crystal.

* philip.allen@stonybrook.edu

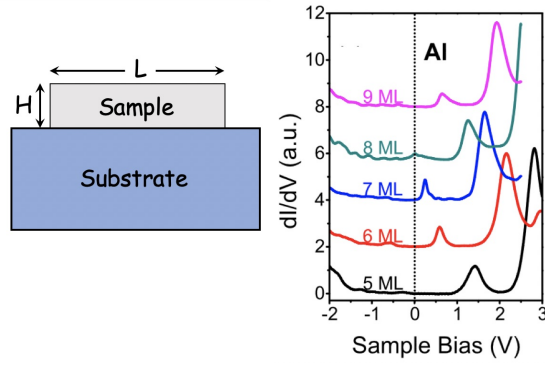


FIG. 1. On the left is a schematic of a film on a substrate. The figure on the right is taken from a paper by Wu *et al.* [12]. They made films of aluminum (Al), carefully grown on a crystalline silicon substrate. The thickness H of those films ranges from 1.2 to 2.1 nm. The horizontal (x and y) dimensions L are many times larger. The measurement shows features that change as the number of Al monolayers (ML) increases. An extension of the free electron picture gives a qualitative and very useful explanation of this behavior, as will be discussed in later sections.

For simplicity, let all atoms be identical, with one atom per unit cell, at locations $\vec{\ell} = n_a \vec{a} + n_b \vec{b} + n_c \vec{c}$, where n_α are integers in the range $1 \leq n_\alpha \leq N$. Thus there are N^3 atoms. The vectors $\vec{a}, \vec{b}, \vec{c}$ define the edges of the crystal's "unit cell". Each atom has Z "free" electrons (*e.g.* 1 for alkali metals like Na, K, \dots ; 3 for Al, Ga, *etc.*); so there are Z electrons per unit cell. The unit cell has volume $V_{\text{cell}} = \vec{a} \cdot (\vec{b} \times \vec{c})$. Then there are $n_{\text{el}} = Z/V_{\text{cell}}$ (potentially free) electrons per unit volume.

It is physically impossible, but mathematically sensible, to have N^3 regularly spaced atoms in a finite volume V with no boundaries. The mathematical trick is to re-imagine the volume as a 3-dimensional torus. For clarity, and later use in metal films, consider first a corresponding one or two dimensional perfect finite crystal. In one dimension, the chain of N atoms with spacing $|\vec{a}| = a$ is mapped onto a circle of circumference $Na = L$. The circle is a 1-dimensional torus. The point $r + Na$ on the circle is the same as the point r , so $\psi_k(r + Na)$ must equal $\psi_k(r)$. This constrains $\exp(ikNa)$ to be 1, so the one-dimensional k -vector is quantized in the form $k = 2\pi m/Na$ where m can be any integer. The number of k -states with $-\pi/a \leq k < \pi/a$ is N , the same as the number of atoms in the 1d crystal. If the number of atoms N is increased, the density of k states increases, so that the maximum occupied energy is unchanged. The states ψ_k are otherwise unaffected by the boundary.

The smallest N k -vectors ($-\pi/a \leq k < \pi/a$) define the one-dimensional version of the "Brillouin zone" (BZ). When k lies outside the BZ, it is a close relative of a state $k - G$ inside the BZ, where $G = 2\pi m/a$ for integer m , and G is referred to as a "reciprocal lattice vector". "Close relative" means that when $\psi_{\vec{k}}$ is evaluated only at atomic positions $\vec{r} = \vec{\ell}$, any value of \vec{k} outside the BZ can be replaced by a vector $\vec{k} + \vec{G}$ inside the BZ without altering $\psi_{\vec{k}}$ at atomic positions. The definition of \vec{G} for dimension > 1 will be given soon.

In two dimensions, the torus is a doughnut, tiled by N^2 parallelograms of sides \vec{a} and \vec{b} . The coordinate $\vec{r} + N\vec{a}$ is the same as \vec{r} , so $\psi_{\vec{k}}(\vec{r} + N\vec{a})$ is the same as $\psi_{\vec{k}}(\vec{r})$, and similarly for \vec{b} . This places two constraints on \vec{k} . Define a vector \vec{A} to have $\vec{A} \cdot \vec{a} = 2\pi$ and direction perpendicular to \vec{b} ($\vec{A} \cdot \vec{b} = 0$). Similarly, define \vec{B} to have $\vec{B} \cdot \vec{b} = 2\pi$ and direction perpendicular to \vec{a} . The periodic constraints $\exp(iN\vec{k} \cdot \vec{a}) = \exp(iN\vec{k} \cdot \vec{b}) = 1$ are satisfied if the k -vector is quantized as $\vec{k} = (m_A \vec{A} + m_B \vec{B})/N$. The number of \vec{k} -states in the parallelogram of sides \vec{A} and \vec{B} is N^2 , the same as the number of atoms in the idealized 2-d crystal. This parallelogram is the Brillouin zone (BZ) in two dimensions.

Similar arguments for 3-d crystals are given in all introductory texts. The unit cell has volume $V_{\text{cell}} = (\vec{a} \times \vec{b}) \cdot \vec{c}$, and the crystal has N^3 atoms in volume $V = N^3 V_{\text{cell}}$. Periodic BC's are the constraint $\psi_{\vec{k}}(\vec{r} + N\vec{a}) = \psi_{\vec{k}}(\vec{r})$, and similarly for translations by $N\vec{b}$ and $N\vec{c}$. This puts three constraints on the \vec{k} -vectors. Choose three primitive \vec{k} -vectors, $\vec{A}, \vec{B}, \vec{C}$, where

$$\vec{A} = 2\pi \frac{\vec{b} \times \vec{c}}{V_{\text{cell}}}; \quad \vec{B} = 2\pi \frac{\vec{c} \times \vec{a}}{V_{\text{cell}}}; \quad \vec{C} = 2\pi \frac{\vec{a} \times \vec{b}}{V_{\text{cell}}}. \quad (3)$$

Then $\vec{A} \cdot \vec{a} = 2\pi$ and $\vec{A} \cdot \vec{b} = \vec{A} \cdot \vec{c} = 0$, and similarly for \vec{B} and \vec{C} . These are the "primitive" reciprocal lattice vectors. The vectors

$$\vec{G} = n_A \vec{A} + n_B \vec{B} + n_C \vec{C} \quad (4)$$

for any integers n_A, n_B, n_C , are the *reciprocal lattice vectors*. The three special vectors $\vec{A}, \vec{B}, \vec{C}$ define a primitive cell in \vec{k} -space, the "Brillouin zone" (BZ). Any \vec{k} -vector outside the BZ can be uniquely related to a vector $\vec{k} + \vec{G}$ inside the BZ, by the fact that both of these vectors share the same phase factor $e^{i\vec{k} \cdot \vec{\ell}} = e^{i(\vec{k} + \vec{G}) \cdot \vec{\ell}}$ under translation by a lattice vector $\vec{\ell}$. The states $\psi_{\vec{k}}(\vec{r})$ and $\psi_{\vec{k} + \vec{G}}(\vec{r})$ behave the same way under translations by $\vec{\ell}$ in spite of being different plane-waves.

The BZ has volume $V_{\text{BZ}} = \vec{A} \cdot (\vec{B} \times \vec{C}) = (2\pi)^3/V_{\text{cell}}$. This uses the identity

$$\vec{a} \cdot (\vec{b} \times \vec{c}) = \frac{(2\pi)^3}{\vec{A} \cdot (\vec{B} \times \vec{C})}. \quad (5)$$

With these definitions, there is a simple definition of the plane waves $\psi_{\vec{k}}$ that obey the periodic BC's. Define \vec{k} to have the form

$$\vec{k} \equiv \frac{1}{N}(n_A \vec{A} + n_B \vec{B} + n_C \vec{C}). \quad (6)$$

Then

$$\psi_{\vec{k}}(\vec{r} + N\vec{a}) = e^{2\pi i n_A} \psi_{\vec{k}}(\vec{r}) = \psi_{\vec{k}}(\vec{r}), \quad (7)$$

and similarly for translations by $N\vec{b}$ and $N\vec{c}$. The integers n_A, n_B, n_C are unrestricted. For any allowed \vec{k} (*i.e.* satisfying Eq. 6), the plane-wave state $\psi_{\vec{k}}(\vec{r})$ obeys periodic BC's. The set of N^3 \vec{k} -vectors inside the parallelepiped defined by $\vec{A}, \vec{B}, \vec{C}$ defines the 3-d BZ. Each \vec{k} -point in the BZ has its own set of phase factors under translations by $\vec{\ell}$. The \vec{k} -vectors in the BZ exhaust all the allowed phase factors. Normally the Brillouin zone is chosen to be centered around the wavevector $\vec{k} = 0$, but any other center gives a shifted BZ with wavevectors having the same complete set of phase factors.

In all dimensions d , the size of the unit cell in \vec{r} -space multiplied by the size of the primitive cell in \vec{k} -space (the Brillouin zone) is $(2\pi)^d$,

$$V_r^{(d)} = \frac{(2\pi)^d}{V_k^{(d)}}. \quad (8)$$

“Size” here means length in 1d, area in 2d, and volume in 3d; it is denoted as $V_r^{(d)}$, or usually just V_d or V .

III. FREE ELECTRONS

For free electrons, the Fermi wavevector k_F is the radius of the object (line, circle, sphere in $d = 1, 2, 3$) that contains all the \vec{k} -points occupied at $T = 0$. For monatomic crystals,

$$V_{k,\text{FS}}^{(d)} = \frac{Z}{2} V_k^{(d)} = \frac{Z}{2} \frac{(2\pi)^d}{V_r^{(d)}} = \frac{n_d}{2} (2\pi)^d, \quad (9)$$

where $n_d = Z/V_r^{(d)}$ is the density of electrons. The factor 1/2 in Eq. 9 accounts for equal occupancy of both spin states. The Fermi wavevector

k_F in $d = 1, 2, 3$ is then

$$\begin{aligned} 2k_F &= \pi n_1 \text{ or } k_F = \frac{\pi}{2} n_1 \text{ in } d = 1 \\ \pi k_F^2 &= 2\pi^2 n_2 \text{ or } k_F = (2\pi n_2)^{1/2} \text{ in } d = 2 \\ \frac{4\pi}{3} k_F^3 &= 4\pi^3 n_3 \text{ or } k_F = (3\pi^2 n_3)^{1/3} \text{ in } d = 3 \end{aligned} \quad (10)$$

where the left hand side of each is $V_{k,\text{FS}}^{(d)}$, the k -space size of the Fermi surface in dimension d .

As an example, consider an idealized 1-d chain of N monovalent atoms, like Na or K. The length of the chain is $L = Na$, where the nearest neighbor distance a is roughly twice the radius of the outer s -state of the neutral atom. In vacuum, the outermost s -electron is weakly bound, and in the chain, it is essentially released. In first approximation, charge is ignored, because the positive charge of the ions left behind and the negative charge of the electrons are assumed to cancel each other. The N free electrons each occupy a spin up or down state $\psi_k = e^{ikx}/\sqrt{L}$. The lowest energy configuration has $N/2$ doubly occupied k -states. Because $Z = 1$, the BZ is half-filled. The $N/2$ doubly occupied states have $-\pi/2a \leq k \leq +\pi/2a$, or $-k_F \leq k \leq +k_F$ where $k_F = \pi/2a$ is the Fermi wavevector. The highest energy of the occupied states is $\epsilon_F = \hbar^2 k_F^2/2m$, the Fermi energy.

If atoms are divalent, they release two electrons, and there are N doubly occupied states. The Fermi wavevector of the 1-d chain is now $k_F = \pi/a$, filling the BZ. Trivalent atoms releasing three free electrons have $k_F = 3\pi/2a$, filling the “first BZ” and half-filling the next one.

IV. NEARLY FREE ELECTRONS

In reality, outer electrons of atoms in a crystal are not truly free. They interact with the ions and with each other. The exact quantum many-body states $\Psi(\vec{r}_1, \vec{r}_2, \dots)$ are too complex to either compute or use. A trick for dealing with this, called the “empirical pseudopotential method”, was developed [14] in the 1960's. The many-body wavefunction is approximated by an antisymmetrized sum of products of one-electron states. Then a carefully constructed approximate one-electron Schroedinger equation is written:

$$\left[\frac{p^2}{2m} + V_{\text{ps}}(\vec{r}) \right] \psi_{\vec{k}}(\vec{r}) = \epsilon_{\vec{k}} \psi_{\vec{k}}(\vec{r}) \quad (11)$$

The Fourier representation of the “pseudopotential” V_{ps} is

$$V_{\text{ps}}(\vec{r}) = \sum_{\vec{G}} V_{\text{ps}}(\vec{G}) e^{i\vec{G}\cdot\vec{r}}, \quad (12)$$

where the Fourier coefficients $V_{\text{ps}}(\vec{G})$ are adjusted using experimental data. The potential has the periodicity of the lattice because the vectors \vec{G} are reciprocal lattice vectors. This empirical method is now less used, because sophisticated semi-empirical procedures (*e.g.* “density-functional theory” or DFT) have been developed which enable an effective one-electron potential $V(\vec{r})$ to be computed without adjustable parameters. Application to Al surfaces is given in Ref. 15. However, the old empirical method gives equally good or better results if fitted well to good experiments, especially for the so-called “simple metals” (Na, Mg, Al, Pb, *etc.*, with only s or p valence electrons). For these, the pseudopotential is small, *i.e.* $|V_{\text{ps}}(\vec{G})|/\epsilon_F \sim 0.2$ or less.

A. One dimensional crystals

To simplify even further, consider the truncated Schroedinger equation

$$\left[\frac{p^2}{2m} + V_{\text{ps}}(e^{2\pi ix/a} + e^{-2\pi ix/a}) \right] \psi_k(x) = E_k \psi_k(x). \quad (13)$$

This is a one-dimensional version of Eqs. 11 and 12. The periodic potential is simplified to have only $G = \pm 2\pi/a$, the smallest non-zero reciprocal lattice vectors. The potential oscillates in space as $\cos(2\pi x/a)$ with a small coefficient $2V_{\text{ps}}$. Start from the non-interacting (plane wave) states ψ_k , the 1-d version of Eq. 1. Then perturbation theory says the energy becomes $E_k = \epsilon_k + \Delta\epsilon_k$. When the shift is small, second-order perturbation theory gives the answer

$$\Delta\epsilon_k = \sum_{G=\pm 2\pi/a} \frac{|V_{\text{ps}}(G)|^2}{\frac{\hbar^2}{2m} [k^2 - (k+G)^2]}. \quad (14)$$

This is small as long as the denominator isn’t too small. When $k = \pm G/2 = \pm\pi/a$, one of the two denominators vanishes, and a more accurate solution is needed. The exact solution for $k = \pi/a$ (and $\epsilon_{\pi/a} = (\hbar\pi/a)^2/2m$) is

$$E_{\pi/a} = \epsilon_{\pi/a} \pm V_{\text{ps}}, \quad (15)$$

and the same for $k = -\pi/a$.

The full answer is illustrated in Fig. 2. In the case $Z = 1$, the occupied states occupy the region from $k = 0$ to $k = \pi/2a$, half-way to the

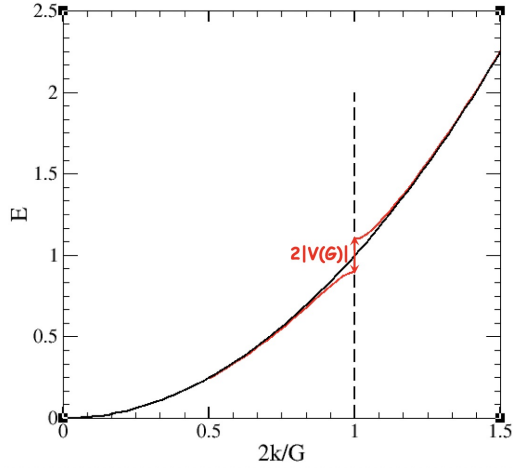


FIG. 2. Free and nearly free electrons in 1d. Free electrons have $\epsilon_k \propto k^2$. The dashed vertical line is the Brillouin zone boundary at $k=G/2$, where nearly free electrons have a gap $\Delta E = 2|V_{\text{ps}}|$. The vertical axis is electron energy in units of $\hbar^2(G/2)^2/2m$. The pseudopotential $V_{\text{ps}} = V(k = G)$ was chosen to have magnitude 0.1 in the same units.

Brillouin zone (BZ) boundary at $G/2 = \pi/a$. The free electron approximation describes the occupied states very well. For $Z = 2$, the occupied states fill the BZ. It is no longer a metal, but an insulator with a gap $2V_{\text{ps}}$. The free electron approximation no longer works for low energy excitations. For $Z = 3$, the occupied states have a Fermi surface at $k = 3\pi/a$, half-way beyond the first BZ boundary; the free electron approximation is fine for electrons near the Fermi energy, but fails for deeper lying states. Most properties will be correctly described by free electrons for 1d chains of atoms with Z loosely bound electrons, except when Z is even, in which case the weak pseudopotential is sufficient to make an insulator.

B. Two dimensional crystals

Unlike $d = 1$, actual samples of monolayers and thin films with $d = 2$ are becoming available thanks to recent advances in synthesis. An actual 2d monolayer (a metal, unlike graphene) is likely to have a triangular lattice. This is the structure of a single layer of an hexagonal close packed (hcp) crystal, or a single layer perpendicular to the (111) direction of a face-centered cubic (fcc) crystal. Translation vectors can be chosen as

$$\vec{a} = a \left(\frac{\sqrt{3}}{2}, -\frac{1}{2} \right) \text{ and } \vec{b} = a \left(\frac{\sqrt{3}}{2}, +\frac{1}{2} \right), \quad (16)$$

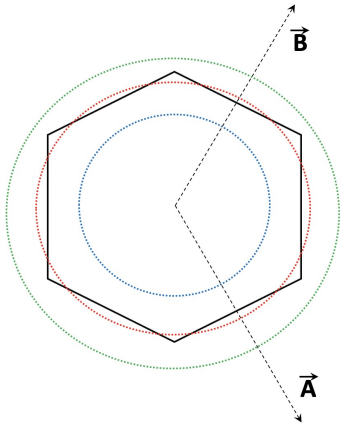


FIG. 3. Free electrons in 2d have circular Fermi surfaces. The hexagon is the surface of the Brillouin zone of a triangular close-packed 2-d lattice, with reciprocal lattice vectors \vec{A} and \vec{B} . The blue, red, and green circles are Fermi circles for $Z = 1, 2,$ and 3 electrons per atom.

where $a = |\vec{a}| = |\vec{b}|$ is the nearest-neighbor distance. The vectors \vec{a} and \vec{b} are 60° apart in the \hat{x} , \hat{y} plane. There is one atom per $2d$ primitive cell, at positions $\vec{\ell} = n_a \vec{a} + n_b \vec{b}$. The corresponding reciprocal lattice vectors are

$$\vec{A} = \frac{4\pi}{\sqrt{3}a} \left(\frac{1}{2}, -\frac{\sqrt{3}}{2} \right) \text{ and } \vec{B} = \frac{4\pi}{\sqrt{3}a} \left(\frac{1}{2}, +\frac{\sqrt{3}}{2} \right) \quad (17)$$

The BZ is a hexagon with edges perpendicular to the midpoint of reciprocal lattice vectors like \vec{A} and \vec{B} , as shown in Fig. 3. The shortest distance to the BZ boundary is $|\vec{A}|/2 = 2\pi/\sqrt{3}a$, or 1.1547 in units of π/a . The longest is 1.3333 in units of π/a . The area of the unit cell is $\sqrt{3}a^2/2$. From Eq. 10, the Fermi wavevector (in units of π/a) is 0.857 ($Z=1$), 1.2125 ($Z=2$), and 1.4850 ($Z=3$). Just as in $d = 1$, a $2d$ monovalent metal should have a Fermi surface (in this case, a circle) unaffected by a weak pseudopotential, and a trivalent metal should have states near the Fermi surface unaffected. The Fermi circle of a $2d$ metal with $Z = 2$ intersects the BZ boundary at 12 points, deforming the Fermi surface. However, most of the points on this deformed Fermi surface may still be nearly free electron states with a small deformation $\Delta\vec{k}$ away from a Fermi circle.

C. Three dimensional crystals

Typical metals that are reasonably well described by a free electron model are Na, Mg, Al and Pb with $Z=1,2,3,$ and 4 . Al and Pb have

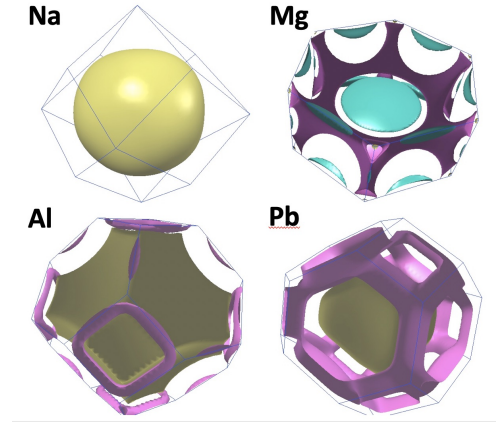


FIG. 4. Free electrons in 3d have spherical Fermi surfaces. Sodium with $Z = 1$ has a body-centered cubic crystal structure with $Z = 1$ electron per unit cell. Its Fermi sphere fits inside its BZ. The other three metals shown have $Z = 2, 3, 4$ and Fermi spheres that intersect the surface of their BZ's. Magnesium has an hexagonal close-packed crystal structure with two atoms (and $2Z = 4$ electrons) in the unit cell. Aluminum and lead have face-centered cubic (fcc) structures with $Z = 3$ or 4 electrons in the unit cell. Figures are from ref. 16.

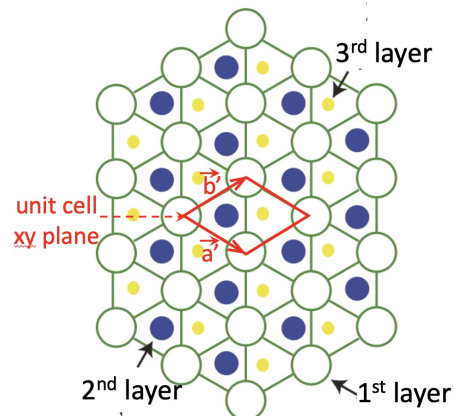


FIG. 5. Three (111) layers of an fcc crystal. The nearest neighbor distance is $a = |\vec{a}'| = |\vec{b}'|$. Layers 2 and 3 (blue and yellow atoms) lie at distances $h = \sqrt{2}/3a$ and $2h$ above layer 1. Image adopted from ref. 17.

fcc structure, with 4 atoms in a cube of volume $(\sqrt{2}a)^3$, where $\sqrt{2}a$ is the cubic lattice constant. The Fermi surfaces are shown in Fig. 4.

V. SIMPLIFIED PICTURES OF FREE ELECTRONS IN SLABS

Free-electron descriptions of metal slabs have often been published, for example, in Refs. 18–

22. The example used in this paper is a slab of six layers ($n_L = 6$) of aluminum. It is an idealized piece of a single (face-centered cubic, fcc) crystal, sliced parallel to the (111) plane. The plane is labeled (111) because it is perpendicular to the $(x, y, z) = (1, 1, 1)$ direction of the cubic crystal. Each layer of the slab is a plane of triangular close packed atoms, arranged in rhombic unit cells described by Eq. 16. The atoms are at positions $\vec{\ell} = n_a \vec{a} + n_b \vec{b}$. The second and third layers are identical to the first, except shifted by $1/3$ and $2/3$ of the diagonal $(\vec{a} + \vec{b})$ of the rhombic cell. The fourth layer is exactly on top of the first layer. The layer spacing in the \hat{z} direction, for the fcc structure, is $\sqrt{2/3}a$, where a denotes the nearest neighbor distance (not the cubic lattice constant which is $\sqrt{2}a$). The slab layer spacing will relax slightly near the surface, but this is hard to measure or compute and is ignored here for simplicity. A 2d projection is shown in Fig. 5. A 3-dimensional repeat unit, with one atom per cell, has translation vectors

$$\begin{aligned} \vec{a}' &= a \left(\frac{\sqrt{3}}{2} \hat{x} - \frac{1}{2} \hat{y} \right) & \vec{b}' &= a \left(\frac{\sqrt{3}}{2} \hat{x} + \frac{1}{2} \hat{y} \right) \\ \text{and } \vec{c}' &= \frac{1}{3} (\vec{a} + \vec{b} + \sqrt{6}a\hat{z}). \end{aligned} \quad (18)$$

There are several ways to choose electron wavefunctions for a slab that are related to the free electron wavefunctions of bulk crystals. Three will now be illustrated:

A. The method closest to the bulk description uses periodic BC's. It differs from bulk results because, while there are many cells (N^2) in the \vec{a} , \vec{b} plane, there is a small number n_L in the perpendicular direction. The quantization of (k_x, k_y) is very dense, but k_z -quantization is sparse.

B. An improvement replaces periodic BC's with hard-wall BC's. The potential is a square-well in the \hat{z} -direction with infinite sides.

C. A further improvement uses a square well with finite sides so that electrons interior to the well can be emitted to the vacuum if given enough energy.

A. Slab with Periodic boundary conditions

When treating bulk free electron systems, the crystal is described as if it had dimensions $N\vec{a}$, $N\vec{b}$, and $N\vec{c}$. The number N is large. A compromise is needed when doing computations; often N^3 is taken to be as small as 10^6 . For (111) films, the dimensions are $N\vec{a}'$, $N\vec{b}'$, and $n_L\vec{c}'$, where n_L , the actual number of layers in the film, is

small. It is convenient to use a choice of reciprocal lattice vectors slightly different from Eq. 3, and more like Eq. 17,

$$\begin{aligned} \vec{A}' &= \frac{4\pi}{\sqrt{3}a} \left(\frac{1}{2} \hat{x} - \frac{\sqrt{3}}{2} \hat{y} \right), & \vec{B}' &= \frac{4\pi}{\sqrt{3}a} \left(\frac{1}{2} \hat{x} + \frac{\sqrt{3}}{2} \hat{y} \right) \\ \text{and } \vec{C}' &= \sqrt{\frac{3}{2}} \frac{2\pi}{a} \hat{z}. \end{aligned} \quad (19)$$

These vectors obey $\vec{A}' \cdot \vec{a}' = 2\pi$, $\vec{A}' \cdot \vec{b}' = 0$, etc. Quantization of \vec{k} -vectors is described by

$$\begin{aligned} \vec{k} &= \vec{k}_{\parallel} + \vec{k}_{\perp}, \text{ where} \\ \vec{k}_{\parallel} &= \frac{1}{N} (n_A \vec{A}' + n_B \vec{B}') \text{ and } \vec{k}_{\perp} = \frac{1}{n_L} (n_C \vec{C}'). \end{aligned} \quad (20)$$

The vectors \vec{k}_{\parallel} are very dense in the xy plane, while the vectors \vec{k}_{\perp} are discrete and well spaced in the z direction. The free electron plane-wave states $\psi_{\vec{k}}$ factorize as

$$\psi_{\vec{k}, \text{PBC}}(\vec{r}) = \frac{1}{\sqrt{V}} e^{i\vec{k}_{\parallel} \cdot \vec{r}_{\parallel}} \times e^{ik_{\perp}z} \quad (21)$$

These are a complete basis of states $\psi_{\vec{k}}$. They have energy

$$\epsilon_{\vec{k}, \text{PBC}} = \epsilon_{\vec{k}_{\parallel}} + \frac{\hbar^2}{2m} \left(\frac{2\pi}{H} \right)^2 n_c^2 \quad (22)$$

where $H = \sqrt{2/3}n_L a = 14.03\text{\AA}$ is the width of the 6-layer slab. The discrete energies proportional to n_c^2 (where $n_c = \dots, -2, -1, 0, 1, 2, \dots$) split the free electron band ($\propto k^2$) into separate two-dimensional bands, each $\propto k_{\parallel}^2$, and separated in energy. The separated bands of a slab are often called "quantum well states" (QWS).

For a 6-layer film of (111) aluminum, the occupied states are contained in a region of \vec{k} -space shown in Fig. 6. Each discrete value of \vec{k}_{\perp} has an infinite two-dimensional (k_x, k_y) plane of corresponding \vec{k}_{\parallel} 's. The occupied states are in circular pieces whose radii $k_{F,n}$ reduce as $|n|$ increases. In first approximation, the radii are fixed by $\hbar^2 k_{F,n}^2 / 2m + \epsilon_{\perp}(n_c) = \epsilon_F$, where $\epsilon_{\perp}(n_c)$ is the second term of Eq. 22, and ϵ_F is the bulk Fermi energy. However, the slab Fermi energy differs a bit from the bulk Fermi energy. To compute $\epsilon_{F, \text{slab}}$, guess the maximum value of n for which $\epsilon_n < \epsilon_F$, and then sum over n_c to compute what value of $\epsilon_{F, \text{slab}}$ gives the correct total number of occupied states. The computation has to be repeated for different guesses of the maximum n until everything is self-consistent. For the six layer slab of Al, using periodic BC's, there are 7

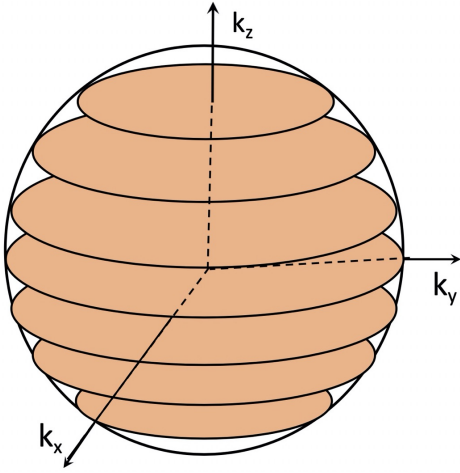


FIG. 6. The “Fermi surface” of a 6 layer slab of (111) sheets of Al, with periodic BC’s. The occupied states lie on circular sheets stacked at values of $k_z = n(2\pi/H)$ where n goes from -3 to 3, and H is the slab thickness, set to 6 times the layer spacing. The “Fermi surface” is the set of 7 circles. The (purely symbolic) sphere is close to the free electron Fermi surface of bulk Al. When the number of layers increases, the number of circles in the sphere increases. In the bulk limit, the circles are so dense that the occupied states are correctly viewed as filling the free electron Fermi sphere.

partially occupied slabs (n_c goes from -3 to +3). The Fermi wavevector for the $n = 0$ central slab is increased by 0.3% compared to bulk and the Fermi energy (the same for all k_z -layers) is increased by 0.6%.

B. Slab with Hard Walls

Periodic BC’s give discrete bands of k -states of the slab. The discreteness is correct, but details are wrong. The main error is that it gives discrete waves $e^{i\vec{k}_\parallel \cdot \vec{r}_\parallel} e^{ik_\perp z}$ which propagate (incorrectly) in the \hat{z} direction as well as correctly in the \hat{x}, \hat{y} directions. A more realistic alternative is “hard-wall” BC’s. An implementation is given by Trivedi and Ashcroft [19].

Instead of using wavefunctions with periodicity H in the z -direction, imagine instead that there is a confining potential,

$$V_{\text{HW}}(z) = \begin{cases} 0, & \text{if } 0 < z < H, \\ \infty, & \text{otherwise.} \end{cases} \quad (23)$$

The Schroedinger equation is

$$\mathcal{H}\psi = \left[\frac{p^2}{2m} + V_{\text{HW}}(z) \right] \psi = E\psi. \quad (24)$$

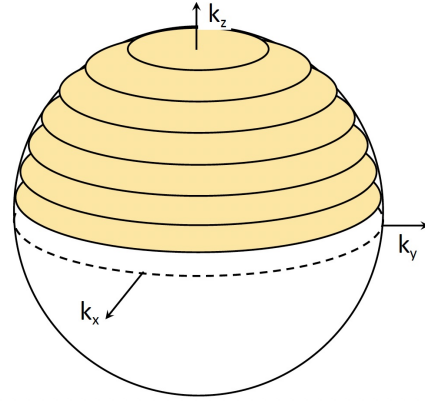


FIG. 7. The “Fermi surface” of a 6 layer slab of (111) sheets of Al, with hard-wall BC’s. The occupied states lie on the yellow circular sheets stacked at values of k_z equal to $n(\pi/H)$ where n goes from 1 to 7, and H is 6 times the layer spacing. The Fermi surface is the set of 7 circles. When the number of layers increases, the number of circles increases. In the bulk limit, the circles are so dense that the occupied states essentially fill the upper half of the free electron Fermi sphere. The spacing of the k_z layers is smaller by 2 than in the previous figure. A more realistic figure of the same type is in Fig. 1 of Ref. 23.

The solutions are

$$\psi_{\vec{k}_\parallel, n}^{\text{HW}}(\vec{r}) = \sqrt{\frac{2}{V}} e^{i\vec{k}_\parallel \cdot \vec{r}_\parallel} \times \sin\left(\frac{n\pi z}{H}\right), \quad (25)$$

where $n = 1, 2, \dots$. The factor of $\sqrt{2}$ appears because the integral of $|\sin(n\pi/z)|^2$ is half as big as the integral of $|e^{ik_\perp z}|^2$. The factor $n\pi/H$ is k_\perp . However, it does not propagate in the z direction; it is a standing wave. The energies are

$$\epsilon_{\vec{k}_\parallel, n, \text{HW}} = \epsilon_{\vec{k}_\parallel} + \frac{\hbar^2}{2m} \left(\frac{\pi}{H}\right)^2 n^2. \quad (26)$$

For even values of n , the energies are the same as in Eq. 22; odd values of n have energies between; and, unlike for periodic BC’s where n_C can be positive, negative, or 0, for hard-wall BC’s, only positive (and non-zero) values of n are permitted.

Results are shown in Fig. 7. The method of hard-wall BC’s brings the free-electron picture a step closer to reality than the fully periodic BC method. A further improvement is discussed in the next section.

C. Soft Walls Surrounded by Vacuum

The work function of the (111) surface of Al is $\Phi(111)=4.26$ eV [24]. Electron states with energy less than $\Phi(111)$ above the Fermi level ϵ_F^{slab}

are confined in the slab. Higher energy electrons will escape, if initially inside the slab, unless they relax down to lower energy confined states. The work function is measured as the minimum photon energy $\hbar\omega$ which can eject an electron from the material. In an Al film, an electron at the Fermi energy ϵ_F^{slab} can be ejected if $\hbar\omega > \Phi(111)$. An electron initially outside and directed toward the slab, will penetrate a bit, and then either be reflected back out or temporarily absorbed. To extend the free-electron model to cover these cases, replace the hard walls of the slab by soft walls. Previously, the position $z = 0$ was at the lower surface of the slab. Now it is more convenient to choose $z = 0$ to be at the center of the slab.

$$V_{\text{SW}}(z) = \begin{cases} 0 & \text{if } |z| < H/2, \\ U_0 & \text{otherwise,} \end{cases} \quad (27)$$

where

$$U_0 = \epsilon_{F,\text{slab}} + \Phi(111). \quad (28)$$

The solutions $\psi_{\vec{k}}(\vec{r}, z) = \exp(i\vec{k}_{\parallel} \cdot \vec{r})u(z)$ have wave-vectors \vec{k}_{\parallel} parallel to the plane. The boundary condition, that ψ is continuous at the slab edges $z = \pm H/2$, requires the wavevector \vec{k}_{\parallel} to be the same both inside and outside the slab.

1. Confined states

Electrons with energy less than U_0 are confined, but have finite, exponentially decaying, amplitudes outside the slab. The wavefunctions are

$$\begin{aligned} \psi_{\vec{k}_{\parallel}}^{\text{conf}} &\propto \begin{cases} e^{i\vec{k}_{\parallel} \cdot \vec{r}_{\parallel}} \sin(k_{\perp}^{\text{SW}} z) & (\text{odd}) \\ e^{i\vec{k}_{\parallel} \cdot \vec{r}_{\parallel}} \cos(k_{\perp}^{\text{SW}} z) & (\text{even}) \end{cases} \\ &\text{if } |z| \leq H/2, \text{ and} \\ \psi_{\vec{k}_{\parallel}}^{\text{conf}} &\propto e^{i\vec{k}_{\parallel} \cdot \vec{r}_{\parallel}} e^{-\lambda(|z| - H/2)} \\ &\text{if } |z| > H/2 \end{aligned} \quad (29)$$

This generalizes the wavefunctions in Eq. 25. However, the wavenumbers were easily found to be $k_{\perp}^{\text{HW}} = n\pi/H$ in the hard-wall case, but the soft-wall wavenumbers k_{\perp}^{SW} need more careful application of the boundary conditions. The answers are similar in both cases, as is shown in Table I.

The wavefunctions in Eq. 29 have energies determined by the Schroedinger equation $(p^2/2m + V_{\text{SW}})\psi_{\text{SW}} = E\psi_{\text{SW}}$, where

$$E - \frac{(\hbar k_{\parallel})^2}{2m} = \begin{cases} \frac{(\hbar k_{\perp}^{\text{SW}})^2}{2m} & \text{if } |z| < H/2 \\ U_0 - \frac{(\hbar\lambda)^2}{2m} & \text{otherwise} \end{cases} \quad (30)$$

where $U_0 = \epsilon_{F,\text{slab}} + \Phi(111)$

n	k_{\perp}^{HW}	$\epsilon_{\perp}^{\text{HW}}$	k_{\perp}^{SW}	$\epsilon_{\perp}^{\text{SW}}$
1	0.64	0.19	0.60	0.17
2	1.28	0.76	1.20	0.67
3	1.92	1.72	1.80	1.50
4	2.57	3.06	2.39	2.66
5	3.21	4.78	2.99	4.15
6	3.85	6.88	3.58	5.96
7	4.49	9.37	4.17	8.07
8	5.13	12.24	4.74	10.46
9	5.77	15.49	5.31	13.09
10	6.41	19.12	5.81	15.70

TABLE I. For the 6-layer Al(111) slab, these are the perpendicular wavenumbers and energies for the first 10 hard-wall (HW), and all the confined soft-wall (SW) cases.

The equality of E inside and outside gives one relation, $(k_{\perp}^{\text{SW}})^2 + \lambda^2 = 2mU_0/\hbar^2$, between the wavenumber k_{\perp}^{SW} and the damping λ . A second relation comes from continuity of ψ_{SW} and $d\psi_{\text{SW}}/dz$ at the walls. This permits both k_{\perp}^{SW} and λ to be fixed. There are multiple solutions, labeled by n , similar to the hard-wall case. For hard walls $k_{\perp} = n\pi/W$, and any integer $n > 0$ is allowed. The soft-wall case has a further restriction, that the energy E of the states of Eqs. 29,30 cannot exceed the energy of the vacuum, $U_0 = \epsilon_{F,\text{slab}} + \Phi(111)$. There are a finite number of such states n . There are infinitely many additional states with $E > U_0$, but they are not damped by $e^{-\lambda|z|}$, because they are unconfined, *i.e.* truly free outside the slab. Equation 29 does not apply; they are discussed in the next section.

For the 6-layer Al(111) case, using the bulk Fermi energy (11.62 eV) and the measured work function ($\Phi(111)=4.26\text{eV}$), there are 10 solutions. The lowest energy solutions have energies and wavefunctions quite close to the hard-wall solutions. This is shown in Table I. By the fifth highest solution, the differences are quite noticeable. This is illustrated in Fig. 8. Figure 9 shows the energies of all 10 soft-wall states, and the corresponding hard-wall states. In the hard-wall case, solutions with higher integers n continue for $n \rightarrow \infty$, but are not shown because their energies are beyond the top of the graph.

The soft-wall method extends free-electron theory as far as it can go in thin slabs, unless more accurate (and more complicated) potentials $V(z)$ are known. Sophisticated one-electron theory, at great computational expense, can produce 3-dimensional potentials $V(x, y, z)$ for a slab, or a film grown on a surface. Then in principle, the x - and y -dependences could be averaged out, to get an accurate $V(z)$. But if the 3-

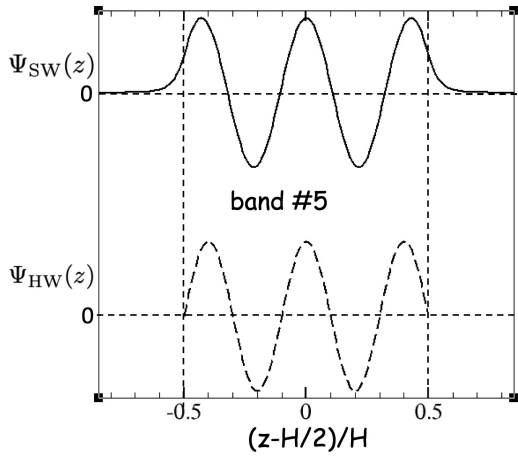


FIG. 8. Wavefunctions of band $n = 5$ for hard-wall boundary conditions (dashed) and soft-wall boundary conditions (solid line).

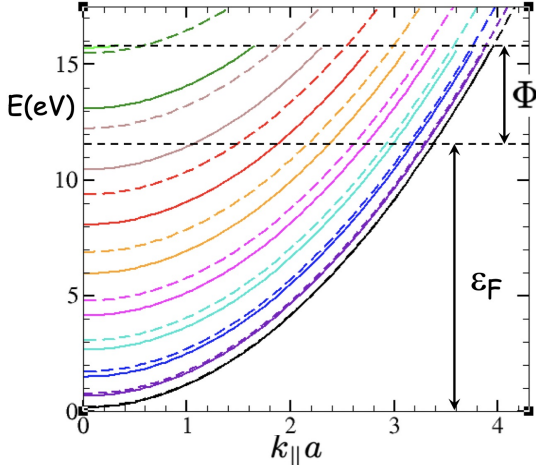


FIG. 9. Hard-wall (dashed curves) and soft-wall (solid curves) electron energies as a function of the 2-dimensional wavevector $k_{\parallel} = |\vec{k}_{\parallel}|$. The soft-wall energies terminate at the energy of the upper dashed line at $U_0 = \epsilon_F + \Phi = 15.87$ eV. Beyond that energy, there are vacuum states which may penetrate the slab but are not described by the same equations. The energies colored black are $n = 1$, maroon are $n = 2$, blue are $n = 3$, etc. For $n=1$ or 2, hard- and soft-wall states are almost indistinguishable. The 10th soft-wall state is just below the vacuum level, barely visible at the upper left. The 10th and higher hard-wall states are above the top of the graph.

dimensional potential is available, the full wavefunctions $\psi(x, y, z)$, and corresponding energies, would have been found during the computation of the potential. There would be little motivation or need for a free-electron theory.

2. Unconfined states

From the Schroedinger eqn. 24, the unconfined states with $E > U_0$ have wavefunctions

$$\psi_{\vec{k}_{\parallel}}^{\text{unconf}} = \begin{cases} C_{\text{in}} e^{i\vec{k}_{\parallel} \cdot \vec{r}_{\parallel}} e^{ik_{\perp}^{\text{in}} z} & \text{if } |z| < H/2 \\ C_{\text{out}} e^{i\vec{k}_{\parallel} \cdot \vec{r}_{\parallel}} e^{ik_{\perp}^{\text{out}} z} & \text{otherwise.} \end{cases} \quad (31)$$

The component \vec{k}_{\parallel} of the wavevector parallel to the slab is the same both inside and outside the slab. The component k_{\perp} has different values, k_{\perp}^{in} and k_{\perp}^{out} . The energy $E(\vec{k})$ has different forms inside and outside of the slab:

$$E(\vec{k}) = \frac{(\hbar k_{\parallel})^2}{2m} + \begin{cases} \frac{(\hbar k_{\perp}^{\text{in}})^2}{2m} \\ U_0 + \frac{(\hbar k_{\perp}^{\text{out}})^2}{2m} \end{cases} \quad (32)$$

The equality of $E(\vec{k})$ inside and outside gives the relation,

$$(k_{\perp}^{\text{in}})^2 - (k_{\perp}^{\text{out}})^2 = 2mU_0/\hbar^2, \quad (33)$$

between the perpendicular wavenumbers k_{\perp}^{in} inside, and k_{\perp}^{out} outside the slab.

Unlike the case of confined states, the wavevector inside, k_{\perp}^{in} , is not constrained by the width H of the slab; it takes essentially continuous values. More precisely, the full system is considered, for normalization purposes, to lie in a finite volume $V = L^3$. The slab is pictured as occupying the center ($-H/2 < z < H/2$) of the space in the z direction ($-L/2 < z < L/2$). Periodic boundary conditions give \vec{k}_{\parallel} the values $2\pi n_x/L$ and $2\pi n_y/L$ in the x and y directions, and k_{\perp}^{out} the values $2\pi n_z/L$. The wavevector k_{\perp}^{in} is then fixed by Eq. 33. The coefficient C_{out} , to lowest order in H/L , is $\sqrt{1/V}$, and the coefficient C_{in} is similar in size, but depends on k_{\perp}^{in} and k_{\perp}^{out} in a complicated way that depends on matching ψ at the boundaries.

3. Unconfined standing waves

The states ψ^{unconf} , both inside and outside, have E independent of the signs of \vec{k}_{\parallel} and k_{\perp} , so the complete wavefunction can consist of a variety of linear combinations of simple waves. The next section deals with waves incident on the slab from outside. This section deals with a symmetric standing wave, which illuminates the states nicely, but is not easy to realize experimentally. The wavefunction has the form

$$\begin{aligned} \psi_{\text{in}} &= \frac{A}{\sqrt{V}} e^{i\vec{k}_{\parallel} \cdot \vec{r}} \cos(k_{\perp}^{\text{in}} z) \\ \psi_{\text{out}} &= \frac{1}{\sqrt{V}} e^{i\vec{k}_{\parallel} \cdot \vec{r}} \cos(k_{\perp}^{\text{out}} z \pm \phi), \end{aligned} \quad (34)$$

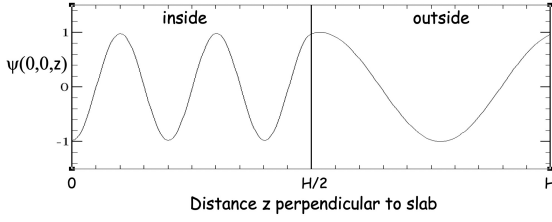


FIG. 10. The symmetric standing-wave wavefunction (Eq. 34) for the state with energy 3eV higher than the vacuum energy U_0 . The slab goes from $z = -H/2$ to $z = H/2$. The sample volume V is replaced by 1.

where ψ_{in} has $|z| < H/2$ and ψ_{out} has $|z| > H/2$. The coefficients A and ϕ are real numbers to be fixed by boundary conditions. The plus sign on ϕ is used for $z > H/2$, and the minus sign for $z < -H/2$. Continuity of ψ and $d\psi/dz$ across the boundaries gives the two equations necessary to determine A and ϕ ,

$$\begin{aligned} A \cos(k_{\perp}^{\text{in}} H/2) &= \cos(k_{\perp}^{\text{out}} H/2 + \phi), \\ A k_{\perp}^{\text{in}} \sin(k_{\perp}^{\text{in}} H/2) &= k_{\perp}^{\text{out}} \sin(k_{\perp}^{\text{out}} H/2 + \phi). \end{aligned} \quad (35)$$

The ratio of these equations eliminates A and gives the equation for the phase ϕ ,

$$k_{\perp}^{\text{in}} \tan(k_{\perp}^{\text{in}} H/2) = k_{\perp}^{\text{out}} \tan(k_{\perp}^{\text{out}} H/2 + \phi) \quad (36)$$

To illustrate this, consider a state with energy 3eV above the vacuum level $U_0=15.9$ eV. The energy is $E=18.9\text{eV}=(\hbar^2 k_{\perp}^{\text{in}})^2/2m$, which gives $k_{\perp}^{\text{in}} H/2 = 15.6$. Then from Eq. 33, $k_{\perp}^{\text{out}} H/2 = 6.22$. Equation 36 then gives $\phi = -6.44$, and Eq. 35 gives $A = -0.980$. The wavefunction is shown in Fig. 10.

4. Unconfined external incident waves

Fabrication of free-standing thin slabs (like the present example of Al) is making rapid progress, largely thanks to advances in imaging of surfaces. One way to examine such a slab is to probe with a monochromatic electron beam. An electron incident from the left has an amplitude T for being transmitted, and R for being reflected from the surface at $z = -H/2$. The transmitted electron wave then travels inside, and has an amplitude T' for being transmitted out through the surface at $z = +H/2$ and R' for being reflected back in the slab. It will then either be transmitted into the vacuum at $z < -H/2$ or reflected again back into the slab. The final result is described by a wavefunction $\psi(z)$ which is a right-moving traveling wave in the right-hand

vacuum ($z > H/2$) and a mix of left- and right-moving traveling waves in the other regions. For an incident wave traveling in the positive z direction ($k_{\perp}^{\text{out}} > 0$ and $\vec{k}_{\parallel} = 0$), the wavefunction is

$$\psi(z) \propto e^{i\vec{k}_{\parallel} \cdot \vec{r}} \begin{cases} e^{ik_{\perp}^{\text{out}} z} + \mathcal{R}e^{-ik_{\perp}^{\text{out}} z} & \text{if } z < -H/2 \\ \mathcal{A}e^{ik_{\perp}^{\text{in}} z} + \mathcal{B}e^{-ik_{\perp}^{\text{in}} z} & \text{if } |z| < H/2 \\ \mathcal{T}e^{ik_{\perp}^{\text{out}} z} & \text{if } z > H/2 \end{cases} \quad (37)$$

There are four boundary conditions that determine the four unknowns ($\mathcal{A}, \mathcal{B}, \mathcal{R}, \mathcal{T}$), namely continuity of ψ and $d\psi/dz$ at $z = -H/2$ and at $z = +H/2$. These give the four equations

$$\begin{aligned} e^{-ik'H/2} + \mathcal{R}e^{ik'H/2} &= \mathcal{A}e^{-ikH/2} + \mathcal{B}e^{ikH/2} \\ e^{-ik'H/2} - \mathcal{R}e^{ik'H/2} &= \frac{k}{k'} [\mathcal{A}e^{-ikH/2} - \mathcal{B}e^{ikH/2}] \\ \mathcal{T}e^{ik'H/2} &= \mathcal{A}e^{ikH/2} + \mathcal{B}e^{-ikH/2} \\ \mathcal{T}e^{ik'H/2} &= \frac{k}{k'} [\mathcal{A}e^{ikH/2} - \mathcal{B}e^{-ikH/2}] \end{aligned} \quad (38)$$

Here a simplified notation uses $k = k_{\perp}^{\text{in}}$ and $k' = k_{\perp}^{\text{out}}$. Adding the first and the second equations gives an equation involving only the two unknowns \mathcal{A}, \mathcal{B} . Subtracting the third from the fourth gives another such equation. Solving the two linear equations gives

$$\begin{aligned} \mathcal{A} &= 2e^{-i(k+k')H/2}/(1 - k/k')\mathcal{D} \\ \mathcal{B} &= -2e^{i(k-k')H/2}/(1 + k/k')\mathcal{D} \\ \mathcal{D} &= +\frac{k - k'}{k + k'}e^{ikH} - \frac{k + k'}{k - k'}e^{-ikH}. \end{aligned} \quad (39)$$

The remaining two unknowns \mathcal{R}, \mathcal{T} can then be evaluated,

$$\begin{aligned} \mathcal{R} &= -e^{-ik'H} + \frac{2}{\mathcal{D}} \left[\frac{e^{-i(k+k')H}}{1 - k/k'} - \frac{e^{i(k-k')H}}{1 + k/k'} \right] \\ \mathcal{T} &= \frac{2}{\mathcal{D}} e^{-ik'H} \left[\frac{1}{1 - (k/k')} - \frac{1}{1 + (k/k')} \right] \end{aligned} \quad (40)$$

Figure 11 shows the result for ψ from Eqs. 39 and 40, using the same energy as in the standing wave of Fig. 10, namely 3eV above the vacuum energy. The real part of ψ (the solid black curve of Fig. 11) is very similar to the standing wave of Fig. 10.

VI. SUMMARY

Bulk crystals have surfaces which can be ignored when thinking about bulk properties like electrical and thermal conductivity. The low energy bulk properties of “simple” metals (those

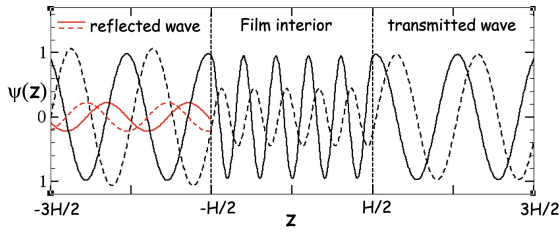


FIG. 11. The wavefunction (Eq. 37, ignoring the x, y dependence) when a plane wave with energy $3eV$ higher than the vacuum energy U_0 is incident from the left, perpendicular to the slab. The black solid and dashed curves are the real and imaginary parts of the total wave. The red solid and dashed curves are the real and imaginary parts of the reflected wave.

with only s and p electrons near the Fermi level) conform reasonably well with the standard free electron model. However, their surfaces are important for many other considerations, and have properties (*e.g.* surface states) outside the scope of a free electron picture.

Crystalline thin films differ in some ways from their bulk versions. Low energy properties of

films of “simple” metals are modified by not having electron propagation in the perpendicular (z) direction. Instead, there are “quantum well states” (QWS) whose nature is not badly described by modifying the free electron theory appropriately. The simplest modification, using periodic boundary conditions in the z direction, while unrealistic, gives a sensible first approach to the QWS modification of electron states. An almost equally simple modification, confining the z motion by a potential well $V(z)$ with infinite barriers at the film boundaries, improves the correspondence with reality. However, it is still unrealistic except when the Fermi level is not too far above the bottom of the sp bands. A nice further improvement is found if the potential well $V(z)$ has a finite barrier set by the measured work function of the bulk metal.

The resulting free electron picture of metallic films does not describe many of the important complications of real films. However, it gives a good pedagogical introduction to metal films. Comparison of actual properties of films with the free electron model is a good way to start understanding the important further complications.

-
- [1] Paul Drude, “Zür Elektronentheorie der Metalle,” *Annalen der Physik* **306**, 566 (1900).
- [2] A. Sommerfeld, “Zur Elektronentheorie der Metalle auf Grund der Fermischen Statistik,” *Zeitschrift für Physik* **47**, 1 (1928).
- [3] G. K. Binnig and H. Rohrer, “Scanning tunneling microscopy,” *Helv. Phys. Acta* **55**, 726–735 (1982).
- [4] G. K. Binnig and H. Rohrer, “Scanning tunneling microscopy—from birth to adolescence,” *Rev. Mod. Phys.* **59**, 615–625 (1987).
- [5] M. Mudrik, S. S. Cohen, and N. Croitoru, “Electron conductivity of very thin metal films,” *Thin Solid Films* **226**, 140–143 (1993).
- [6] T.-C. Chiang, “Photoemission studies of quantum well states in thin films,” *Surface Science Reports* **39**, 181–235 (2000).
- [7] T. Miller, M. Y. Chou, and T.-C. Chiang, “Phase relations associated with one-dimensional shell effects in thin metal films,” *Phys. Rev. Lett.* **102**, 236803 (2009).
- [8] T. Miller and T.-C. Chiang, “Quantum electronic stability of atomically uniform films,” in *Thin Film Growth*, edited by Zexian Cao (Woodhead Publishing, Cambridge, U.K., 2011) Chap. 2, pp. 22–51.
- [9] M. Milun, P. Pervan, and D. P. Woodruff, “Quantum well structures in thin metal films: simple model physics in reality?” *Reports on Progress in Physics* **65**, 99 (2002).
- [10] W. A. Atkinson and A. J. Slavin, “A free-electron calculation for quantum size effects in the properties of metallic islands on surfaces,” *Am. J. Phys.* **76**, 1099–1101 (2008).
- [11] M. C. Tringides, M. Jalochowski, and E. Bauer, “Quantum size effects in metallic nanostructures,” *Physics Today* **60**, 50–54 (2007).
- [12] Xuefeng Wu, Chaoqiang Xu, Kedong Wang, and Xudong Xiao, “Systematic investigation of pseudogaps in In, Al, and Pb islands,” *Phys. Rev. B* **92**, 035434 (2015).
- [13] M. Born and T. von Karman, “Über Schwingungen im Raumgittern,” *Physikalische Zeitschrift* **13**, 297–309 (1912).
- [14] M. L. Cohen and T. K. Bergstresser, “Band structures and pseudopotential form factors for fourteen semiconductors of the diamond and zinc-blende structures,” *Phys. Rev.* **141**, 789–796 (1966).
- [15] Gui Qin Huang, “Electronic structures, surface phonons, and electron-phonon interactions of Al(100) and Al(111) thin films from density functional perturbation theory,” *Phys. Rev. B* **78**, 214514 (2008).
- [16] T.-S. Choy, J. Naset, S. Hershfield, and C. J. Stanton, (2000), the Fermi surface database, <http://www.phys.ufl.edu/fermisurface>.
- [17] Shree Ram Acharya and Talat S Rahman, “Toward multiscale modeling of thin-film growth processes using SLKMC,” *Journal of Materials Research* **33**, 709–719 (2018).
- [18] F. K. Schulte, “A theory of thin metal films: electron density, potentials and work function,”

- Surface Science **55**, 427–444 (1976).
- [19] N. Trivedi and N. W. Ashcroft, “Quantum size effects in transport properties of metallic films,” Phys. Rev. B **38**, 12298 (1988).
- [20] J. M. Pitarke and A. G. Eguiluz, “Jellium surface energy beyond the local-density approximation: Self-consistent-field calculations,” Phys. Rev. B **63**, 045116 (2001).
- [21] Biao Wu and Zhenyu Zhang, “Stability of metallic thin films studied with a free electron model,” Phys. Rev. B **77**, 035410 (2008).
- [22] Yong Han and Da-Jiang Liu, “Quantum size effects in metal nanofilms: Comparison of an electron-gas model and density functional theory calculations,” Phys. Rev. B **80**, 155404 (2009).
- [23] P. Czoschke, Hawoong Hong, L. Basile, and T.-C. Chiang, “Quantum size effects in the surface energy of Pb/ Si (111) film nanostructures studied by surface x-ray diffraction and model calculations,” Phys. Rev. B **72**, 075402 (2005).
- [24] R. M. Eastment and C. H. B. Mee, “Work function measurements on (100), (110) and (111) surfaces of aluminium,” J. Phys. F: Metal Phys. **3**, 1738 (1973).